Two-Higgs-Doublet type-II and -III models and t ightarrow ch at the LHC

Abdesslam Arhrib, a,b Rachid Benbrik, c,d Chuan-Hung Chen, e Melina Gomez-Bock f and Souad Semlali d

E-mail: aarhrib@ictp.it, rbenbrik@ictp.it, physchen@mail.ncku.edu.tw, melina.gomez@udlap.mx, s.seemlali@gmail.com

ABSTRACT: Based on the updated 8 TeV LHC data for the Higgs searches, we study the constraints of generic two-Higgs-doublet model (2HDM) type-III and the impacts of the new Yukawa couplings. For comparisons, we revisit the analysis in 2HDM type-II. For understanding the influence of all involving free parameters and realizing their correlations, we employ χ -square fitting approach by including theoretical and experimental constraints, such as $B \to X_s \gamma$, $B_q - \bar{B}_q$ mixing, S, T and U oblique parameters, the production of standard model Higgs and its decay to $\gamma\gamma$, WW^*/ZZ^* , $\tau^+\tau^-$, etc. The errors of analysis are taken at 68%, 95.5% and 99.7% confidence level. Due to the new Yukawa couplings being associated with $\cos(\beta - \alpha)$ and $\sin(\beta - \alpha)$, we find that the allowed regions for $\sin \alpha$ and $\tan \beta$ in type-III could be broader when the dictated parameter χ_F is positive; however, for negative χ_F , the limits are more strict than those in type-II model. By using the constrained parameters, we find that the deviation from the SM in $h \to Z\gamma$ could be of $\mathcal{O}(10\%)$. Additionally, we also study the top-quark flavor changing processes induced at the tree level in type-III model and find that when all current experimental data are considered, we get $Br(t \to c(h, H)) < 10^{-3}$ for $m_h = 125.36$ and $m_H = 150$ GeV and $Br(t \to cA)$ slightly exceeds 10^{-3} for $m_A = 130$ GeV.

KEYWORDS: Standard Model, Higgs boson, 2HDM, Top-quark, FCNC.

^a Département de Mathématiques, Faculté des Sciences et Techniques, Université Abdelmalek Essaadi, B. 416, Tangier, Morocco

^bPhysics Division, National Center for Theoretical Sciences, Hsinchu 300, Taiwan

^cFaculty of Polydisciplinaire de Safi, Sidi Bouzid B.P 4162, 46000 Safi, Morocco

^dLPHEA, Faculty of Science Semlalia, Cadi Ayyad University, Marrakesh, Morocco

^eDepartment of Physics, National Cheng-Kung University, Tainan 701, Taiwan

f DAFM, Universidad de las Américas Puebla. Ex. Hda. Sta. Catarina Mártir 72810, Cholula, Pue. México

C	ontents	
1	Introduction	1
2	The Model	2
3	Theoretical and experimental constraints	4
4	Parameter setting, Global fitting and numerical results 4.1 Parameters and global fitting	6
5	Numerical Results	7
6	$t \to ch { m decay}$	11
7	Conclusions	14

1 Introduction

A scalar boson around 125 GeV has been observed in 2012 by ATLAS [1] and CMS [2] at CERN with more than 5σ significance. The discovery of such particle is based on the analyses of following channels: $\gamma\gamma$, WW^* , ZZ^* and $\tau^+\tau^-$ with an error of order of 20-30% and $b\bar{b}$ channel with an error of order of 40-50%. The recent updates from ATLAS and CMS with $7 \oplus 8$ TeV data [3–7] indicate the possible deviations from the standard model (SM) predictions. Although the errors of current data are still somewhat large, however the new physics signals may become clear in the second run of the LHC at 13-14 TeV.

It is expected that the Higgs couplings to gauge bosons (fermions) at the LHC indeed could reach 4-6% (6-13%) accuracy when the collected data are up to the integrated luminosity of 300 fb⁻¹ [8, 9]. Furthermore, e^+e^- Linear Collider (LC) would be able to measure the Higgs couplings at the percent level [10]. Therefore, the goals of LHC at run II are (a) to pin down the nature of the observed scalar and see if it is the SM Higgs boson or a new scalar boson; (b) to reveal the existence of new physics effect, such as the measurement of flavor changing neutral currents (FCNCs) at the top-quark decays, i.e. $t \to qh$.

Motivated by the observations of the diphoton, WW^* , ZZ^* and $\tau^+\tau^-$ processes at ATLAS and CMS, it is interesting to investigate what sorts of models may naturally be consistent with these measurements and what the implications are for other channels, e.g. $h \to Z\gamma$ and $t \to ch$. Although many possible extensions of the SM have been discussed [11, 12], it is interesting to study the simplest extension from one Higgs doublet to two-Higgs-doublet model (2HDM) [13–20]. According to the situation of Higgs fields couplings to fermions, the 2HDMs are classified as type-I, -II, -III, lepton specific model and flipped model. The 2HDM type-III is the case where both Higgs doublets couple to all fermions;

as a result, FCNCs at the tree level occur. The detailed discussions on the 2HDMs could refer to Ref. [15].

After scalar particle of 125 GeV is discovered, the implications of the observed $h \to \gamma\gamma$ in the type-I and II models are studied in Ref. [21] and the impacts on $h \to \gamma Z$ are given in Refs. [22, 23]. As known, $\tan \beta$ and angle α are important free parameters in 2HDMs, where the former is the ratio of two vacuum expectation values (VEVs) of Higgses and the latter is the mixing parameter between the two CP-even scalars. It is found that the current LHC data put rather severe constraints on the free parameters [16]. For instance, the large $\tan \beta \sim m_t/m_b$ scenario in type-I and -II is excluded except if we tune the α parameter to be rather small $\alpha < 0.02$. Nevertheless, both type-I and type-II models could still fit the data in some small region of $\tan \beta$ and α .

In this paper, we will explore the influence of new Higgs couplings on $h \to \tau^+\tau^-$, $h \to gg, \gamma\gamma, WW, ZZ$ and $h \to Z\gamma$ decays in the framework of 2HDM type-III. We will show what is the most favored regions of the type-III parameter space when theoretical and experimental constraints are considered simultaneously. FCNCs of heavy quark such as $t \to qh$ have been intensively studied both from the experimental and theoretical point of view [24]. Such processes are well established in the SM and are excellent probes for the existence of new physics. In the SM and 2HDM type-I and -II, top FCNCs are generated at one loop level by charged currents and are highly suppressed due to GIM mechanism. The branching ratio (BR) for $t \to ch$ in the SM is estimated to be 3×10^{-14} [25]. If this decay $t \to ch$ is observed, it would be an indisputable sign of new physics. Since the FCNCs occur at the tree level in type-III model, we are going to explore if the $Br(t \to ch)$ could reach the order of 10^{-5} – 10^{-4} [26, 27], the sensitivity which is expected by the integrated luminosity of 3000 fb⁻¹.

The paper is organized as follows. In section II, we introduce the scalar potential and the Yukawa interactions in 2HDM type-III. The theoretical and experimental constraints are described in section III. We set up the free parameters and establish the χ -square for the best-fit approach in section VI. In the same section, we discuss the numerical results when all theoretical and experimental constraints are taken into account. The conclusions are given in section V.

2 The Model

In this section we define the scalar potential and the Yukawa sector in the 2HDM type-III. The scalar potential in $SU(2)_L \otimes U(1)_Y$ gauge symmetry and CP invariance is given by [15]:

$$V(\Phi_{1}, \Phi_{2}) = m_{1}^{2} \Phi_{1}^{\dagger} \Phi_{1} + m_{2}^{2} \Phi_{2}^{\dagger} \Phi_{2} - (m_{12}^{2} \Phi_{1}^{\dagger} \Phi_{2} + \text{h.c}) + \frac{1}{2} \lambda_{1} (\Phi_{1}^{\dagger} \Phi_{1})^{2} + \frac{1}{2} \lambda_{2} (\Phi_{2}^{\dagger} \Phi_{2})^{2}$$
$$+ \lambda_{3} (\Phi_{1}^{\dagger} \Phi_{1}) (\Phi_{2}^{\dagger} \Phi_{2}) + \lambda_{4} (\Phi_{1}^{\dagger} \Phi_{2}) (\Phi_{1}^{\dagger} \Phi_{2}) + \frac{1}{2} \lambda_{5} [(\Phi_{1}^{\dagger} \Phi_{2})^{2} + \text{h.c.}] , \qquad (2.1)$$

where the doublets $\Phi_{1,2}$ have weak hypercharge Y = 1, the corresponding VEVs are v_1 and v_2 and λ_i and m_{12} are real parameters. After the electroweak symmetry breaking, three of the eight degrees of freedom in the two Higgs doublets are the Goldstone bosons (G^{\pm}, G^0)

and the remaining five degrees of freedom become the physical Higgs bosons: 2 CP-even h, H, one CP-odd A, and a pair of charged Higgs H^{\pm} . After using the minimized conditions and the W mass, the potential in Eq. (2.1) has seven parameters which will be taken as: $(\lambda_i)_{i=1,\dots,5}$, m_{12} , and $\tan\beta \equiv v_2/v_1$. Equivalently, we can use the masses as the independent parameters, therefore, the set of free parameters can be chosen to be

$$\{m_h, m_H, m_A, m_{H^{\pm}}, \tan \beta, \alpha, m_{12}\},$$
 (2.2)

where the angle β diagonalizes the squared mass matrices of CP-odd and charged scalars and the angle α diagonalizes the CP-even squared-mass matrix. It has been known that by assuming neutral flavor conservation at the tree level [28], we have four types of Higgs couplings to the fermions. In the 2HDM type-I, the quarks and leptons couple only to one of the two Higgs doublets and the case is the same as the SM. In the 2HDM type-II, the charged leptons and down type quarks couple to one Higgs doublet and the up type quarks couple to the other. The lepton-specific model is similar to type-I, but the leptons couple to the other Higgs doublet. In the flipped model, which is similar to type-II, the leptons and up type quarks couple to the same double.

If one allows the FCNCs at the tree level, both doublets would couple to leptons and quarks and the associated model is called 2HDM type-III [15, 29, 30]. The Yukawa interactions for quarks are written as

$$\mathcal{L}_Y = \bar{Q}_L Y^k d_R \phi_k + \bar{Q}_L \tilde{Y}^k u_R \tilde{\phi}_k + h.c.$$
 (2.3)

where the flavor indices are suppressed, $Q_L^T = (u_L, d_L)$ is the left-handed quark doublet, Y^k and \tilde{Y}^k denote the 3×3 Yukawa matrices, $\tilde{\phi}_k = i\sigma_2\phi_k^*$ and k is the doublet number. Similar formulae could be applied to the lepton sector. Since the mass matrices of quarks are combined by $Y^1(\tilde{Y}^1)$ and $Y^2(\tilde{Y}^2)$ for down (up) type quarks, $Y^{1,2}(\tilde{Y}^{1,2})$ generally cannot be diagonalized simultaneously with the quark mass matrices. As a result, FCNCs at tree level would occur and the effects could lead to the oscillations of $K - \bar{K}$, $B_q - \bar{B}_q$ and $D - \bar{D}$ at the tree level. To get naturally small FCNCs, one can use the ansatz formulated by $Y_{ij}^k, \tilde{Y}_{ij}^k \propto \sqrt{m_i m_j}/v$ [29, 30]. After spontaneous symmetry breaking, the scalar couplings to fermions can be expressed by [31]

$$\mathcal{L}_{Y}^{2\text{HDM-III}} = \bar{u}_{Li} \left(\frac{\cos \alpha}{\sin \beta} \frac{m_{u_i}}{v} \delta_{ij} - \frac{\cos(\beta - \alpha)}{\sqrt{2} \sin \beta} X_{ij}^{u} \right) u_{Rj} h
+ \bar{d}_{Li} \left(-\frac{\sin \alpha}{\cos \beta} \frac{m_{d_i}}{v} \delta_{ij} + \frac{\cos(\beta - \alpha)}{\sqrt{2} \cos \beta} X_{ij}^{d} \right) d_{Rj} h
+ \bar{u}_{Li} \left(\frac{\sin \alpha}{\sin \beta} \frac{m_{u_i}}{v} \delta_{ij} + \frac{\sin(\beta - \alpha)}{\sqrt{2} \sin \beta} X_{ij}^{u} \right) u_{Rj} H
+ \bar{d}_{Li} \left(\frac{\cos \alpha}{\cos \beta} \frac{m_{d_i}}{v} \delta_{ij} - \frac{\sin(\beta - \alpha)}{\sqrt{2} \cos \beta} X_{ij}^{d} \right) d_{Rj} H
- i\bar{u}_{Li} \left(\frac{1}{\tan \beta} \frac{m_{u_i}}{v} \delta_{ij} - \frac{X_{ij}^{u}}{\sqrt{2} \sin \beta} \right) u_{Rj} A
+ i\bar{d}_{Li} \left(-\tan \beta \frac{m_{d_i}}{v} \delta_{ij} + \frac{X_{ij}^{d}}{\sqrt{2} \cos \beta} \right) d_{Rj} A + \text{h.c.},$$
(2.4)

where $v = \sqrt{v_1^2 + v_2^2}$, $X_{ij}^q = \sqrt{m_{q_i} m_{q_j}} / v \chi_{ij}^q$ (q = u, d) and χ_{ij}^q are the free parameters. By above formulation, if FCNC effects are ignored, the results are returned to the case of 2HDM type-II, given by

$$\mathcal{L}_{Y}^{2HDM-II} = \bar{u}_{Li} \left(\frac{\cos \alpha}{\sin \beta} \frac{m_{u_i}}{v} \delta_{ij} \right) u_{Rj} h + \bar{d}_{Li} \left(-\frac{\sin \alpha}{\cos \beta} \frac{m_{d_i}}{v} \delta_{ij} \right) d_{Rj} h + \text{h.c.}$$
 (2.5)

For the couplings of other scalars to fermions, one can be referred to Ref. [31]. We see clearly that if $\chi_{ij}^{u,d}$ are of $\mathcal{O}(10^{-1})$, the new effects are dominated by heavy fermions and comparable with those in type-II model. The couplings of h and H to gauge bosons V = W, Z are proportional to $\sin(\beta - \alpha)$ and $\cos(\beta - \alpha)$, respectively. Therefore, the SM-like Higgs boson h is recovered when $\cos(\beta - \alpha) \approx 0$. The decoupling limit can be achieved if $\cos(\beta - \alpha) \approx 0$ and $m_h \ll m_H, m_A, m_{H\pm}$ are satisfied [32]. From Eqs. (2.4) and (2.5), one can also find that in the decoupling limit, the h couplings to quarks are returned to the SM case.

In our analysis, since we take α in the range $-\pi/2 \le \alpha \le \pi/2$, $\sin \alpha$ will have both positive and negative sign. In 2HDM type-II, if $\sin \alpha < 0$ then the Higgs couplings to up and down type quarks will have the same sign as those in the SM. It is worthy to mention that $\sin \alpha$ in minimal supersymmetric SM (MSSM) is negative unless some extremely large radiative corrections flip its sign [32]. If $\sin \alpha$ is positive, then the Higgs coupling to down quarks will have a different sign with respect to the SM case. This is called by the wrong sign Yukawa coupling in the literature [32, 33]. Later we will explain if the type-III model would favor such wrong sign scenario or not.

3 Theoretical and experimental constraints

The free parameters in the scalar potential defined in Eq. (2.1) could be constrained by theoretical requirements and the experimental measurements, where the former mainly includes tree level unitarity and vacuum stability when the electroweak symmetry is broken spontaneously. Since the unitarity constraint involves a variety of scattering processes, we adopt the results obtained by Refs. [34, 35]. We also force the potential to be perturbative by requiring that all quartic couplings of the scalar potential obey $|\lambda_i| \leq 8\pi$ for all *i*. For the vacuum stability conditions which ensure that the potential is bounded from below, we require that the parameters satisfy the conditions as [36, 37]

$$\lambda_1>0\;,\qquad \lambda_2>0\;, \lambda_3+\sqrt{\lambda_1\lambda_2}>0,\quad \sqrt{\lambda_1\lambda_2}+\lambda_3+\lambda_4-|\lambda_5|>0\quad.$$

In the following we state the constraints from experimental data. The new neutral and charged scalar bosons in 2HDM will affect the self-energy of W and Z bosons through the loop effects. Therefore, the involved parameters could be constrained by the precision measurements of the oblique parameters, denoted by S, T and U [38]. Taking $m_h = 125$ GeV, $m_t = 173.3$ GeV and assuming that U = 0, the tolerated ranges for S and T are found by [39]

$$\Delta S = 0.06 \pm 0.09$$
, $\Delta T = 0.10 \pm 0.07$, (3.1)

where the correlation factor is $\rho = +0.91$, $\Delta S = S^{2\text{HDM}} - S^{\text{SM}}$ and $\Delta T = T^{2\text{HDM}} - T^{\text{SM}}$, and their explicit expressions can be found in Ref [32]. We note that in the limit $m_{H^{\pm}} = m_{A^0}$, ΔT vanishes.

The second set of constraints comes from B physics observables. It has been shown recently in Ref. [40] that $Br(\overline{B} \to X_s \gamma)$ gives a lower limit on $m_{H^{\pm}} \ge 480$ GeV in type-II and -III at 95%CL. However, the constraint is not suitable for the type-I and -IV. By the precision measurements of $Z \to b\bar{b}$ and $B_q - \bar{B}_q$ mixing, the values of $\tan \beta < 0.5$ have been excluded [41]. In this work we allow $\tan \beta \ge 0.5$. In addition, except in some very specific scenario, $\tan \beta$ can not be too large due to the requirement of perturbation theory.

By the observation of scalar boson at $m_h \approx 125$ GeV, now the searches for Higgs boson at ATLAS and CMS could also give a strong bound on the free parameters. The signal events in the Higgs measurements are represented by the signal strength, which is defined by the ratio of Higgs signal to the SM prediction and given by

$$\mu_i^f = \frac{\sigma_i(h) \cdot Br(h \to f)}{\sigma_i^{SM}(h) \cdot Br^{SM}(h \to f)} \equiv \bar{\sigma}_i \cdot \mu_f, \qquad (3.2)$$

where $\sigma_i(h)$ denotes the Higgs production cross section by channel i and $Br(h \to f)$ is the BR for the Higgs decay $h \to f$. Since several Higgs boson production channels are available at the LHC, we are interested in the gluon fusion production (ggF), $t\bar{t}h$, vector boson fusion (VBF) and Higgs-strahlung Vh with V = W/Z; and they are grouped to be $\mu^f_{ggF+t\bar{t}h}$ and μ^f_{VBF+Vh} . In order to consider the constraints from the current LHC data, the scaling factors which show the Higgs coupling deviations from the SM are defined as:

$$\kappa_V = \kappa_W = \kappa_Z \equiv \frac{g_{hVV}^{2\text{HDM}}}{g_{hVV}^{\text{SM}}}, \quad \kappa_f \equiv \frac{y_{hff}^{2\text{HDM}}}{y_{hff}^{\text{SM}}},$$
(3.3)

where g_{hVV} and y_{hff} are the Higgs couplings to gauge bosons and fermions, respectively, and f stands for top, bottom quarks and tau lepton. The scaling factors for loop induced channels are defined by

$$\kappa_{\gamma}^{2} \equiv \frac{\Gamma(h \to \gamma \gamma)_{2\text{HDM}}}{\Gamma(h \to \gamma \gamma)_{\text{SM}}}, \quad \kappa_{g}^{2} \equiv \frac{\Gamma(h \to g \, g)_{2\text{HDM}}}{\Gamma(h \to g \, g)_{\text{SM}}},
\kappa_{Z\gamma}^{2} \equiv \frac{\Gamma(h \to Z\gamma)_{2\text{HDM}}}{\Gamma(h \to Z\gamma)_{\text{SM}}}, \quad \kappa_{h}^{2} \equiv \frac{\Gamma(h)_{2\text{HDM}}}{\Gamma(h)_{\text{SM}}},$$
(3.4)

where $\Gamma(h \to XY)$ is the partial decay rate for $h \to XY$. In our study, the partial decay width of the Higgs is taken from [42], where QCD corrections have been taken into account. In the decay modes $h \to \gamma \gamma$ and $h \to Z\gamma$, we have included the contributions of charged Higgs and the effects of new Yukawa couplings. Accordingly, the ratio of cross section to the SM prediction for the production channels $ggF + t\bar{t}h$ and VBF+Vh can be expressed as

$$\overline{\sigma}_{ggF+t\bar{t}h} = \frac{\kappa_g^2 \sigma_{SM}(ggF) + \kappa_t^2 \sigma_{SM}(tth)}{\sigma_{SM}(ggF) + \sigma_{SM}(tth)}, \qquad (3.5)$$

$$\overline{\sigma}_{VBF+Vh} = \frac{\kappa_V^2 \sigma_{SM}(VBF) + \widetilde{\kappa}_{Zh} \widetilde{\sigma}_{SM}(Zh) + \kappa_V^2 \sigma_{SM}(Zh) + \kappa_V^2 \sigma_{SM}(Wh)}{\sigma_{SM}(VBF) + \widetilde{\sigma}_{SM}(Zh) + \sigma_{SM}(Zh) + \sigma_{SM}(Wh)}, \quad (3.6)$$

where $\sigma_{SM}(Zh)$ is from the coupling of ZZh and occurs at the tree level and $\widetilde{\sigma}_{SM}(Zh) \equiv \sigma_{SM}(gg \to Zh)$ represents the effects of top-quark loop. With $m_h = 125.36$ GeV, the scalar factor $\widetilde{\kappa}_{Zh}$ can be written as [3]

$$\widetilde{\kappa}_{Zh} = 2.27\kappa_Z^2 + 0.37\kappa_t^2 - 1.64\kappa_Z\kappa_t. \tag{3.7}$$

In our numerical estimations, we use $m_h = 125.36$ GeV which is from LHC Higgs Cross section Working Group [8] and is obtained at $\sqrt{s} = 8$ TeV. For considering the experimental bounds, the values of signal strengths, combined the results of ATLAS [5] and CMS [43] and denoted by $\hat{\mu}_{qqF+t\bar{t}h}^f$ and $\hat{\mu}_{VBF+Vh}^f$, are shown in Table. 1.

Table 1. Combined best-fit signal strengths $\widehat{\mu}_{ggF+tth}$ and $\widehat{\mu}_{VBF+Vh}$ and correlation coefficient ρ for the Higgs decay mode [5, 43].

f	$\widehat{\mu}_{ ext{ggF+tth}}^f$	$\widehat{\mu}_{\mathrm{VBF+Vh}}^f$	$\pm 1\hat{\sigma}_{ggF+tth}$	$\pm 1 \widehat{\sigma}_{VBF+Vh}$	ρ
$\gamma\gamma$	1.32	0.8	0.38	0.7	-0.30
ZZ^*	1.70	0.3	0.4	1.20	-0.59
WW^*	0.98	1.28	0.28	0.55	-0.20
$\tau\tau$	2	1.24	1.50	0.59	-0.42
$bar{b}$	1.11	0.92	0.65	0.38	0

4 Parameter setting, Global fitting and numerical results

4.1 Parameters and global fitting

After introducing the scaling factors for representing the new physics in various channels, in the following we show the explicit relations with the free parameters in type-III model. By the definitions in Eq. (3.2), the scaling factors for κ_V and κ_f in type-III are given by

$$\kappa_{V} = \sin(\beta - \alpha),
\kappa_{U} = \kappa_{t} = \kappa_{c} = \frac{\cos \alpha}{\sin \beta} - \chi_{F} \frac{\cos(\beta - \alpha)}{\sqrt{2} \sin \beta},
\kappa_{D} = \kappa_{b} = \kappa_{\tau} = -\frac{\sin \alpha}{\cos \beta} + \chi_{F} \frac{\cos(\beta - \alpha)}{\sqrt{2} \cos \beta}.$$
(4.1)

For simplifying the numerical analysis, we have set $\chi_{ij}^u = \chi_{ij}^d = \chi_{ij}^\ell = \chi_F$. In the 2HDM, the charged Higgs will also contribute to $h \to \gamma \gamma$ decay and the associated scalar triplet coupling hH^+H^- is read by

$$\lambda_{hH^{\pm}H^{\mp}} = \frac{1}{2m_W^2} \left(\frac{\cos(\alpha + \beta)}{\sin 2\beta} (2m_h^2 - 2\lambda_5 v^2) - \sin(\beta - \alpha)(m_h^2 - 2m_{H^{\pm}}^2) \right). \tag{4.2}$$

The scaling factors for loop induced processes $h \to (\gamma \gamma, Z\gamma, gg)$ can be expressed by

$$\kappa_{\gamma}^{2} \sim \left| 1.268\kappa_{W} - 0.279\kappa_{t} + 0.0042\kappa_{b} + 0.0034\kappa_{c} + 0.0036\kappa_{\tau} - 0.0014\lambda_{hH^{\pm}H^{\mp}} \right|^{2},$$

$$\kappa_{Z\gamma}^{2} \sim \left| 1.058\kappa_{W} - 0.059\kappa_{t} + 0.00056\kappa_{b} + 0.00014\kappa_{c} - 0.00054\lambda_{hH^{\pm}H^{\mp}} \right|^{2},$$

$$\kappa_{g}^{2} \sim \left| 1.078\kappa_{t} - 0.065\kappa_{b} - 0.013\kappa_{c} \right|^{2},$$
(4.3)

where we have used $m_h = 125.36$ GeV and taken $m_{H^{\pm}} = 480$ GeV. It is clear that the charged Higgs contribution to $h \to \gamma \gamma$ and $h \to Z \gamma$ is small.

In order to study the influence of new free parameters and to understand their correlations, we perform the χ -square fitting by using the LHC data for Higgs searches [1, 2, 4, 6]. For a given channel $f = \gamma \gamma, WW^*, ZZ^*, \tau \tau$, we define the χ_f^2 as

$$\chi_f^2 = \frac{1}{\hat{\sigma}_1^2 (1 - \rho^2)} (\mu_1^f - \hat{\mu}_1^f)^2 + \frac{1}{\hat{\sigma}_1^2 (1 - \rho^2)} (\mu_2^f - \hat{\mu}_2^f)^2 - \frac{2\rho}{\hat{\sigma}_1 \hat{\sigma}_2 (1 - \rho^2)} (\mu_1^f - \hat{\mu}_1^f) (\mu_2^f - \hat{\mu}_2^f) , \quad (4.4)$$

where $\hat{\mu}_{1,2}^f$, $\hat{\sigma}_{1,2}$ and ρ are the measured Higgs signal strengths, their one-sigma errors, and their correlation, respectively and their values could refer to Table 1, the indices 1 and 2 in turn stand for ggF + tth and VBF + Vh, and $\mu_{1,2}^f$ are the results in the 2HDM. The global χ -square is defined by

$$\chi^2 = \sum_f \chi_f^2 + \chi_{ST}^2 \,, \tag{4.5}$$

where the χ^2_{ST} is related to the χ^2 for S and T parameters, the definition can be obtained from Eq.(4.4) by replacing $\mu^f_1 \to S^{2HDM}$ and $\mu^f_2 \to T^{2HDM}$, and the corresponding values can be found from Eq. (3.1). We do not include $b\bar{b}$ channel in our analysis because the errors of data are still large.

In order to display the allowed regions for the parameters, we show the best fit at 68%, 95.5% and 99.7% confidence level (CL), that is, the corresponding error of χ^2 is $\Delta \chi^2 \leq 2.3$, 5.99, 11.8, respectively. For comparing with LHC data, we require the calculated results in agreement with those shown in ATLAS Fig. 3 of Ref. [3] and in CMS Fig. 5 of Ref. [7].

5 Numerical Results

In the following we present the limits of current LHC data based on the three kinds of CL introduced in last section. In our numerical calculations, we set the mass of SM Higgs to be $m_h = 125.36$ GeV and scan the involving parameters in the chosen regions as

$$480 \,\text{GeV} \le m_{H^{\pm}} \le 1 \,\text{TeV}, \quad 126 \,\text{GeV} \le m_H \le 1 \,\text{TeV}, \quad 100 \,\text{GeV} \le m_A \le 1 \,\text{TeV},$$

 $-1 \le \sin \alpha \le 1, \quad 0.5 \le \tan \beta \le 50, \quad -(1000 \,\text{GeV})^2 \le m_{12}^2 \le (1000 \,\text{GeV})^2. \quad (5.1)$

To get the typical contributions from FCNC effects, we adopt $\chi_F = \pm 1$.

In the 2HDM, there involve many new free parameters; for displaying the limits of parameters, we use two important dimensionless parameters $\sin \alpha$ and $\tan \beta$ as the representatives. Based on the settings in Eq. (5.1) and the theoretical and experimental constraints stated earlier, we first present the allowed regions for $\sin \alpha$ and $\tan \beta$ in Fig. 1,

where the left, middle and right panels stand for the 2HDM type-II, type-III with $\chi_F = -1$ and type-III with $\chi_F = +1$, respectively, and in each plot we show the constraints at 68% CL (green), 95.5% CL (red) and 99.7% CL (black). Our results in type-II are consistent with those obtained by the authors in Refs. [16, 21] when the same conditions are chosen. By the plots, we see that in type-III with $\chi_F = -1$, due to the sign of coupling being the same as type-II, the allowed values for $\sin \alpha$ and $\tan \beta$ are further shrunk; especially $\sin \alpha$ is limited to be less than 0.1. On the contrary, type-III with $\chi_F = +1$, the allowed values of $\sin \alpha$ and $\tan \beta$ are broad.

As discussed before, the decoupling limit occurs at $\alpha \to \beta - \pi/2$, i.e. $\sin \alpha = -\cos \beta < 0$. Since we regard the masses of new scalars as free parameters and scan them in the regions shown in Eq. (5.1), therefore, the three plots in Fig. 1 cover lower and heavier mass of charged Higgs. We further check that $\sin \alpha > 0$ could be excluded at 95.5(99.7)% CL when $m_{H^{\pm}} \geq 585(690)$ GeV. The main differences between type-II and type-III are the

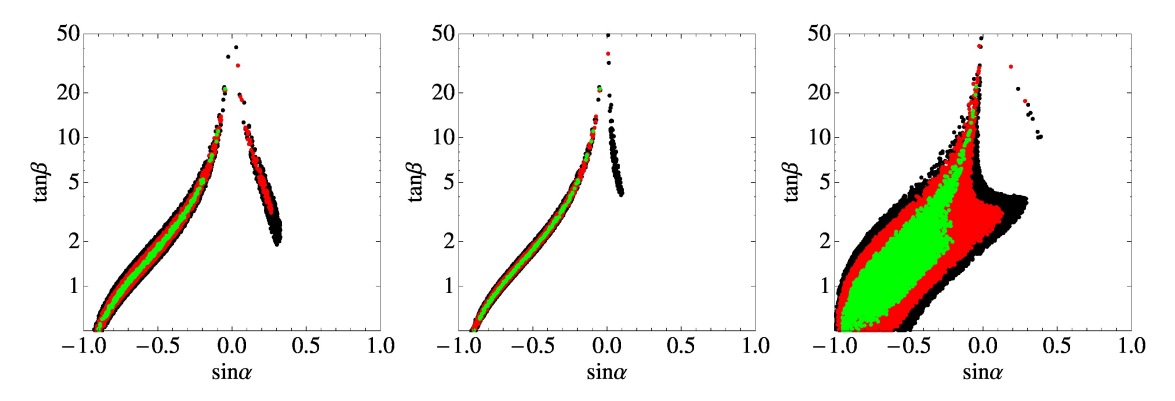


Figure 1. The allowed regions in $(\sin \alpha, \tan \beta)$ constrained by theoretical and current experimental inputs, where we have used $m_h = 125.36$ GeV, the left, middle and right panels stand for the 2HDM type-II, type-III with $\chi_F = -1$ and type-III with $\chi_F = +1$, respectively. The errors for χ -square fit are 99.7% CL (black), 95.5% CL (red) and 68% CL (green).

Yukawa couplings as shown in Eq. (2.4). In order to see the influence of the new effects of type-III, we plot the allowed κ_g as a function of $\sin \alpha$ and $\tan \beta$ in Fig. 2, where the three plots from left to right correspond to type-II, type-III with $\chi_F = -1$ and type-III with $\chi_F = +1$, the solid, dashed and dotted lines in each plot stand for the decoupling limit (DL) of SM, 15% deviation from DL and 20% deviation from DL, respectively. For comparisons, we also put the results of 99.7% in Fig. 1 in each plot. By the analysis, we see that the deviations of κ_g from DL in $\chi_F = +1$ are clear and significant while the influence of $\chi_F = -1$ is small. It is pointed out that a wrong sign Yukawa coupling to down type quarks could happen in type-II 2HDM [32, 33]. For understanding the sign flip, we rewrite the κ_D defined in Eq. (4.1) to be

$$\kappa_D = -\frac{\sin \alpha}{\cos \beta} \left(1 - \frac{\chi_F \sin \beta}{\sqrt{2}} \right) + \frac{\chi_F \cos \alpha}{\sqrt{2}} \,. \tag{5.2}$$

In the type-II case, we know that in the decoupling limit $\kappa_D = 1$, but $\kappa_D < 0$ if $\sin \alpha > 0$. According to the results in the left panel of Fig. 1, $\sin \alpha > 0$ is allowed when the errors

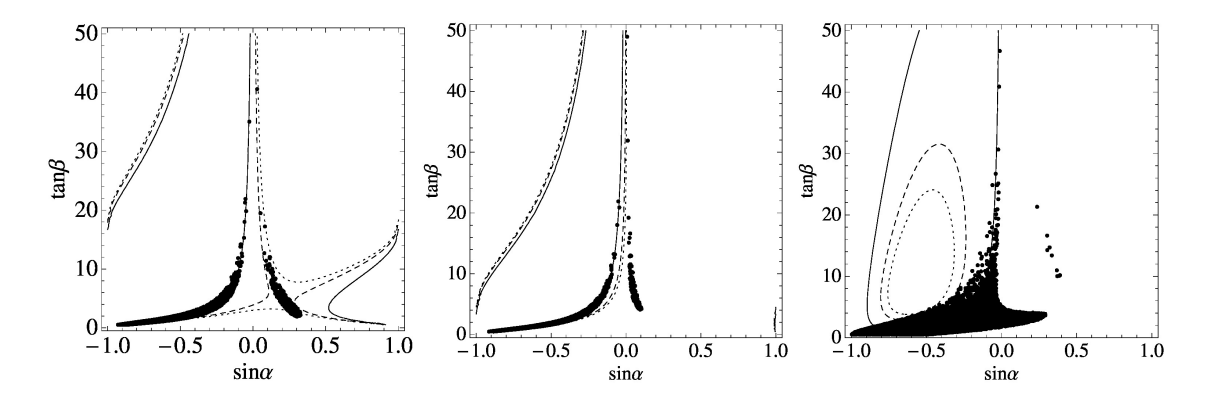


Figure 2. κ_g as a function of $\sin \alpha$ and $\tan \beta$ in type-II (left) and type-III with $\chi_F = (-1, +1)$ (middle, right), where the solid, dashed and dotted lines in each plot stand for the decoupling limit (DL) of SM, 15% deviation from DL and 20% deviation from DL, respectively. The dotted points are the allowed values of parameters resulted from Fig. 1.

of best fit are taken by 2σ or 3σ . The situation in type-III is more complicated. From Eq. (5.2), we see that the factor in the brackets is always positive, therefore, the sign of the first term should be the same as that in type-II case. However, due to $\alpha \in [-\pi/2, \pi/2]$, the sign of the second term in Eq. (5.2) depends on the sign of χ_F . For $\chi_F = -1$, even $\sin \alpha < 0$ in the right sign case, κ_D could be negative when the first term is smaller than the second term. For $\chi_F = +1$, if $\sin \alpha > 0$ and the first term is over the second term, the $\kappa_D < 0$ is still allowed. In order to understand the available values of κ_D when the constraints are considered, we present the correlation of κ_U and κ_D in Fig. 3, where from left to right the panels stand for type-II, type-III with $\chi_F = -1$ and type-III with $\chi_F = +1$. In each plot, the results obtained by χ -square fitting and shown in Fig. 1 are applied. The similar correlation of κ_V and κ_D is presented in Fig. 4. By these results, we find that comparing with type-II model, the negative κ_D gets more strict limit in type-III, although a wider parameter space for $\sin \alpha > 0$ is allowed in type-III with $\chi_F = +1$. Besides the

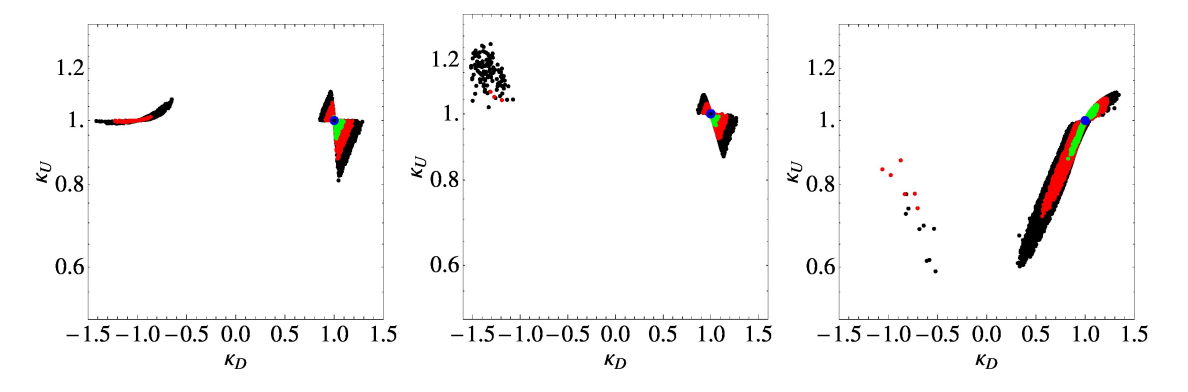


Figure 3. Correlation of κ_D and κ_U , where the left, middle and right panels represent the allowed values in type-II, type-III with $\chi_F = -1$ and type-III with $\chi_F = +1$, respectively and the results of Fig. 1 are applied.

scaling factors of tree level Higgs decays, $\kappa_{D,U}$ and κ_V , it is also interesting to understand

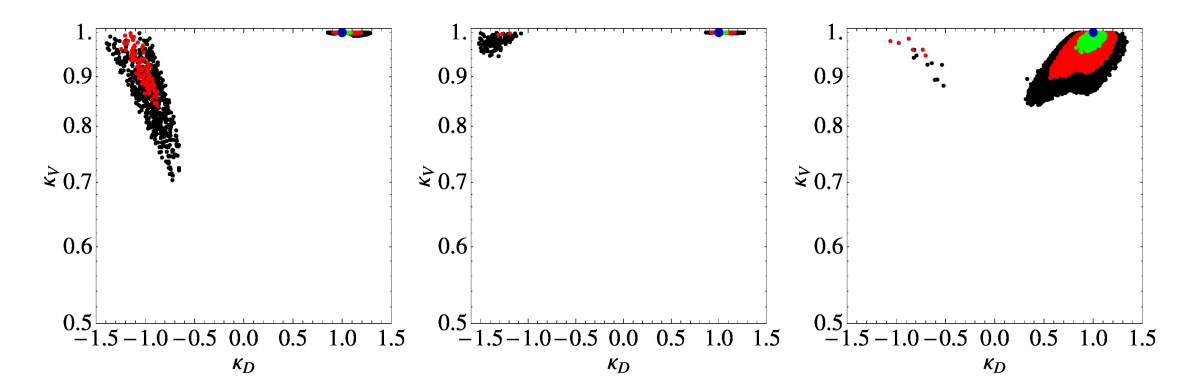


Figure 4. The legend is the same as that in Fig. 3, but for the correlation of κ_V and κ_D .

the allowed values for loop induced processes in 2HDM, e.g. $h \to \gamma\gamma$, gg, and $Z\gamma$, etc. It is known that the differences in the associated couplings between $h \to \gamma\gamma$ and gg are the colorless W-, τ -, and H^{\pm} -loop. By Eq. (4.3), we see that the contributions of τ and H^{\pm} are small, therefore, the main difference is from the W-loop in which the κ_V involves. By using the χ -square fitting approach and with the inputs of the experimental data and theoretical constraints, the allowed regions of κ_{γ} and κ_{g} in type-III and type-III are displayed in Fig. 5, where the panels from left to right are type-II, type-III with $\chi_F = -1$ and +1; the green, red and black colors in each plot stand for the 68%, 95.5% and 99.7% CL, respectively. We find that except a slightly lower κ_{γ} is allowed in type-II, the first two plots have similar results. The situation can be understood from Figs. 3 and 4, where the κ_U in both models is similar while κ_V in type-II could be smaller in the region of negative κ_D ; that is, a smaller κ_V will lead a smaller κ_V . In $\chi_F = +1$ case, the allowed values of κ_{γ} and κ_{g} are localized in a wider region. It is known that except the different gauge couplings, the loop diagrams for

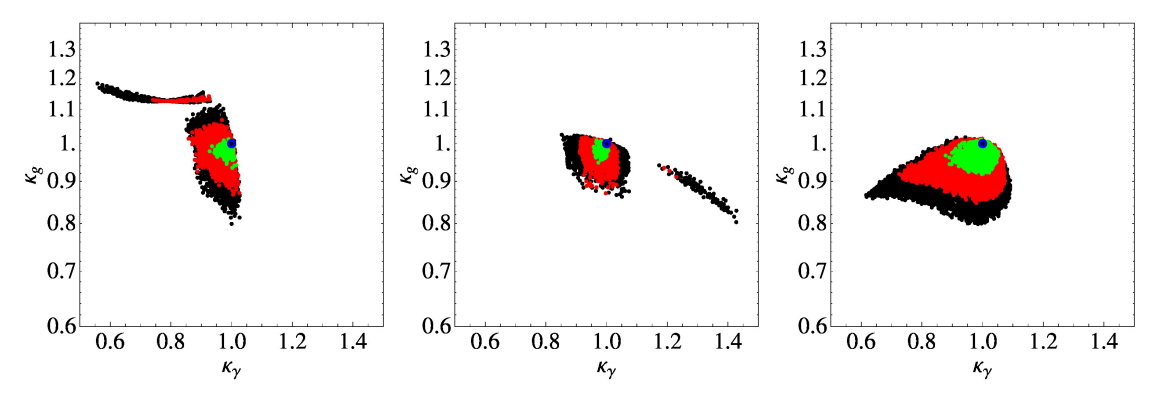


Figure 5. Correlation of κ_{γ} and κ_{g} , where the left, middle and right panels represent the allowed values in type-II, type-III with $\chi_{F} = -1$ and type-III with $\chi_{F} = +1$, respectively and the results in Fig. 1 obtained by χ -square fitting are applied.

 $h \to Z\gamma$ and $h \to \gamma\gamma$ are exact the same. One can realize the loop effects in numerical form from Eq. (4.3). Therefore, we expect the correlation between $\kappa_{Z\gamma}$ and κ_{γ} should behave like a linear relation. We present the correlation between κ_{γ} and $\kappa_{Z\gamma}$ in Fig. 6, where the legend is the same as that for Fig. 5. From the plots, we see that in most region $\kappa_{Z\gamma}$ is less than

the SM prediction. The type-III with $\chi_F = -1$ gets more strict constraint and the change is within 10%. For $\chi_F = +1$, the deviation of $\kappa_{Z\gamma}$ from unity could be over 10%. From run I data, the LHC has an upper bounds on $h \to Z\gamma$, at run II this decay mode will be probed. We give our predictions for LHC at $\sqrt{s} = 13$ TeV for the signal strength $\mu_{ggF+tth}^{\gamma\gamma}$ and $\mu_{ggF+tth}^{Z\gamma}$ in Fig. 7. As results and within the theoretical and experimental constraints applied before, $\mu_{ggF+tth}^{Z\gamma}$ is bounded and could be $\mathcal{O}(10\%)$ far from SM at 68%CL.

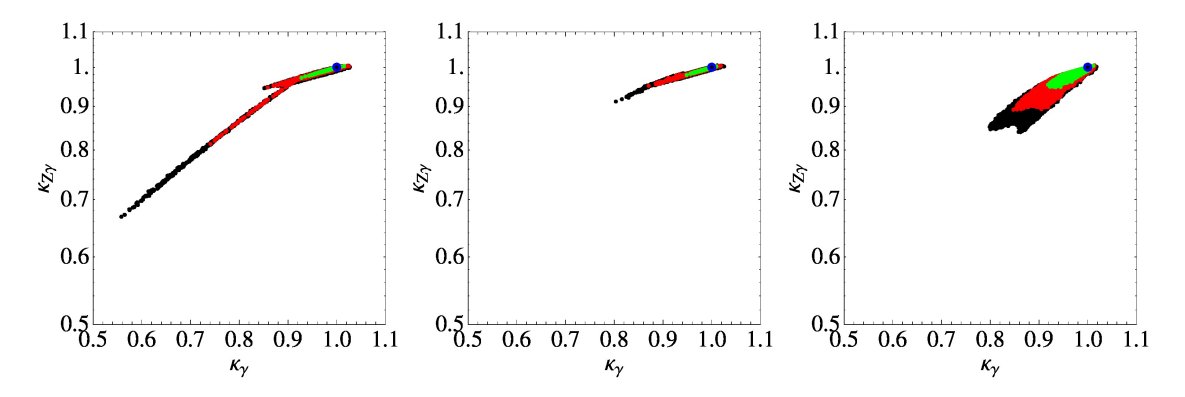


Figure 6. The allowed regions in $(\kappa_{\gamma}, \kappa_{Z\gamma})$ plan after imposing theoretical and experimental constrains. Color coding the same as Fig. 1

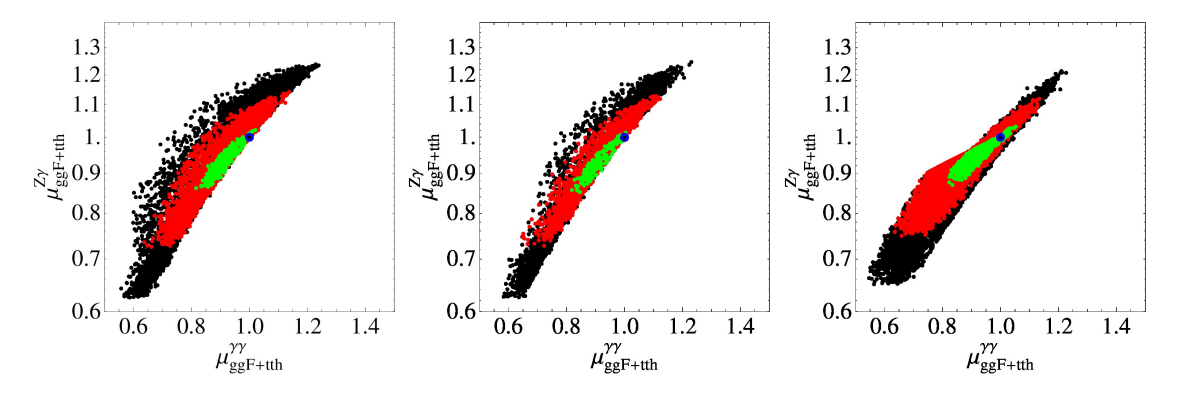


Figure 7. Correlation between $\mu_{ggF+tth}^{\gamma\gamma}$ and $\mu_{ggF+tth}^{Z\gamma}$ at $\sqrt{s}=13$ TeV after imposing theoretical and experimental constrains. Left, middle and right panels represent the allowed values in type-III, type-III with $\chi_F=-1$ and type-III with $\chi_F=+1$, respectively and the results in Fig. 1 obtained by χ -square fitting are applied.

6 $t \rightarrow ch \ decay$

In this section, we study the flavor changing $t \to ch$ process in type-III model. Experimentally, there have been intensive activities to explore the top FCNCs. CDF, D0 and LEPII collaborations have reported some bounds on top FCNCs. At the LHC with rather large top cross section, ATLAS and CMS search for top FCNCs and put a limit on the branching fraction which is $Br(t \to ch) < 0.82$ % for ATLAS [26] and $Br(t \to ch) < 0.56$ % for CMS [27]. Note that CMS limit is slightly better than ATLAS limit. CMS search for $t \to ch$

in different channels: $h \to \gamma \gamma$, WW^* , ZZ^* , and $\tau^+\tau^-$ while ATLAS used only diphoton channel. With the high luminosity option of the LHC, the above limit will be improved to reach about $Br(t \to ch) < 1.5 \times 10^{-4}$ [26] for ATLAS detector.

From the Yukawa couplings in Eq. (2.4), the partial width for $t \to ch$ decay is given by

$$\Gamma(t \to ch) = \left(\frac{\cos(\alpha - \beta)X_{23}^u}{\sin \beta}\right)^2 \frac{m_t}{32\pi} \left((x_c + 1)^2 - x_h^2 \right) \times \sqrt{1 - (x_h - x_c)^2} \sqrt{1 - (x_h + x_c)^2}$$
(6.1)

where $x_c = m_c/m_t$, $x_h = m_h/m_t$ and X^u_{23} is a free parameter and dictates the FCNC effect. It is clear from the above expression that the partial width of $t \to ch$ is proportional to $\cos(\beta - \alpha)$. As seen in the previous section, in the case where h is SM-like, $\cos(\beta - \alpha)$ is constrained by LHC data to be rather small and the $t \to ch$ branching fraction is limited. As we will see later in 2HDM type-II with flavor conservation the rate for $t \to ch$ is much smaller than type-III [45]. Since we assume that the charged Higgs is heavier than 400 GeV, the total decay width of the top contains only $t \to ch$ and $t \to bW$. With $m_h = 125.36$ GeV, $m_t = 173.3$ GeV and $m_c = 1.42$ GeV, the total width can be written as

$$\Gamma_t = \Gamma_t^{SM} + 0.0017 \left(\frac{\cos(\alpha - \beta) X_{23}^u}{\sin \beta} \right)^2 \text{ GeV}$$
 (6.2)

where Γ_t^{SM} is the partial decay rate for $t \to Wb$ and is given by

$$\Gamma_t^{SM} = \frac{G_F m_t^3}{8\pi\sqrt{2}} (1 - \frac{m_W^2}{m_t^2})^2 (1 + 2\frac{m_W^2}{m_t^2}) (1 - 2\frac{\alpha_s(m_t)}{3\pi} (2\frac{\pi^2}{3} - \frac{5}{2})) = 1.43 \,\text{GeV}$$

in which the QCD corrections have been included. By the above numerical expressions together with the current limit from ATLAS and CMS, the limit on the tch FCNC coupling is found by

$$\left(\frac{\cos(\alpha - \beta)X_{23}^u}{\sin \beta}\right) < 2.2 \quad \text{for} \quad Br(t \to ch) < 8.2 \times 10^{-3},$$

$$\left(\frac{\cos(\alpha - \beta)X_{23}^u}{\sin \beta}\right) < 0.36 \quad \text{for} \quad Br(t \to ch) < 5.6 \times 10^{-3} \tag{6.3}$$

in agreement with [46].

We perform a systematic scan over 2HDM parameters, as depicted in Eq. (5.1), taking into account LHC and theoretical constraints. In Fig. 8(left) we illustrate the branching fraction of $t \to ch$ in 2HDM-III as a function of $\cos(\beta - \alpha)$. The LHC constraints within 1σ restrict $\cos(\beta - \alpha)$ to be in the range [-0.27, 0.27]. The branching fraction for $t \to ch$ is slightly above 10^{-4} . The actual CMS and ATLAS constraint on $Br(t \to ch) < 5.6 \times 10^{-3}$ does not restrict $\cos(\beta - \alpha)$. The expected limit from ATLAS detector with high luminosity 3000 fb⁻¹ is depicted as the dashed horizontal line. As one can see, the expected ATLAS limit is somehow similar to LHC constraints within 1σ . In the right panel, we show the allowed parameters space in $(\sin \alpha, \tan \beta)$ plan where we apply ATLAS expected limit $Br(t \to ch) < 1.5 \times 10^{-4}$. This plot should be compared to the right panel of Fig.1. It

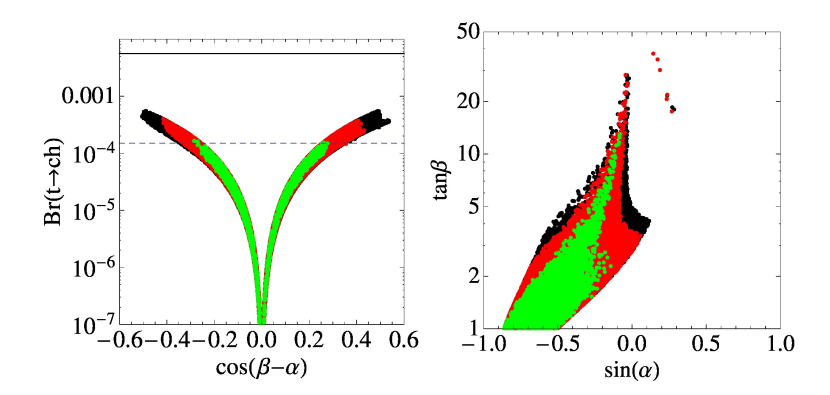


Figure 8. Left: Branching ratio of $Br(t \to ch)$ as a function of $\cos(\beta - \alpha)$, the two horizontal lines correspond to LHC actual limit (upper line) and expected limit from ATLAS with 3000 fb⁻¹ luminosity (dashed line). Right panel: allowed parameters space in type III with the ATLAS expected limit on $Br(t \to ch) < 1.5 \times 10^{-4}$.

is then clear that this additional constraint only act on the 3σ allowed region from LHC data. In Fig. 9 and 10 we show the fitted branching fractions for $t \to ch$ (left), $t \to cH$ at $m_H = 150$ GeV (middle) and $t \to cA$ at $m_A = 130$ GeV (right) as a function of κ_U , where Fig. 9 is for $\chi_F = +1$ while Fig. 10 is $\chi_F = -1$. In the case of $\chi_F = +1$ the fitted value for κ_U at the 3σ level is in the range [0.6, 1.18] and the branching fraction for $t \to ch$, cH are less than 10^{-3} while $Br(t \to cA)$ slightly exceed the 10^{-3} level. Similarly, for $\chi_F = -1$ the fitted value for κ_U at the 3σ level is in the range [0.85, 1.25] and the branching fraction for $t \to ch$, cH, cA are the same size as in the previous case.

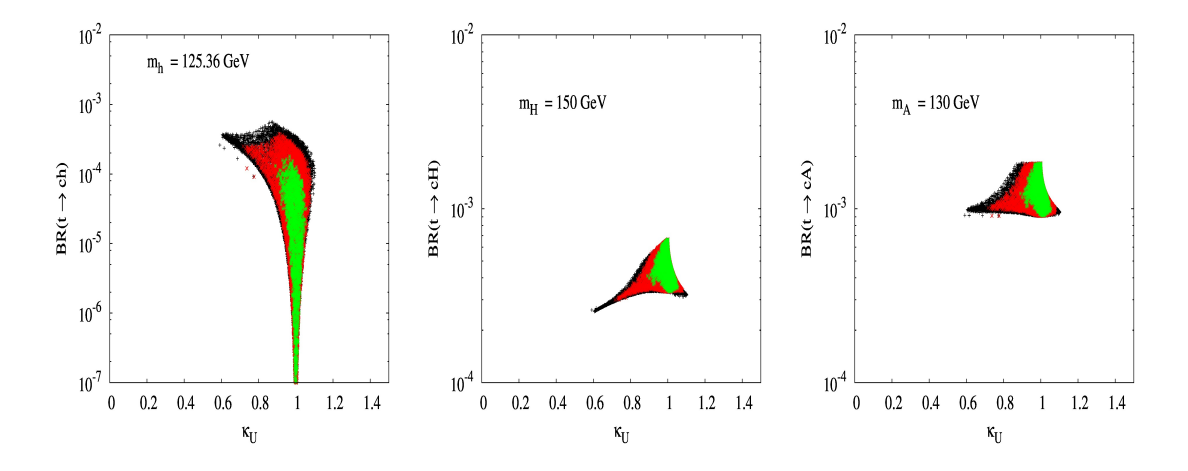


Figure 9. Branching ratios of $Br(t \to ch)(left)$, $Br(t \to cH)(middle)$ and $Br(t \to ch)(right)$ as a function of κ_U in type III with $\chi_F = +1$. For $m_h = 125.36$ GeV, $m_H = 150$ GeV and $m_A = 130$ GeV.

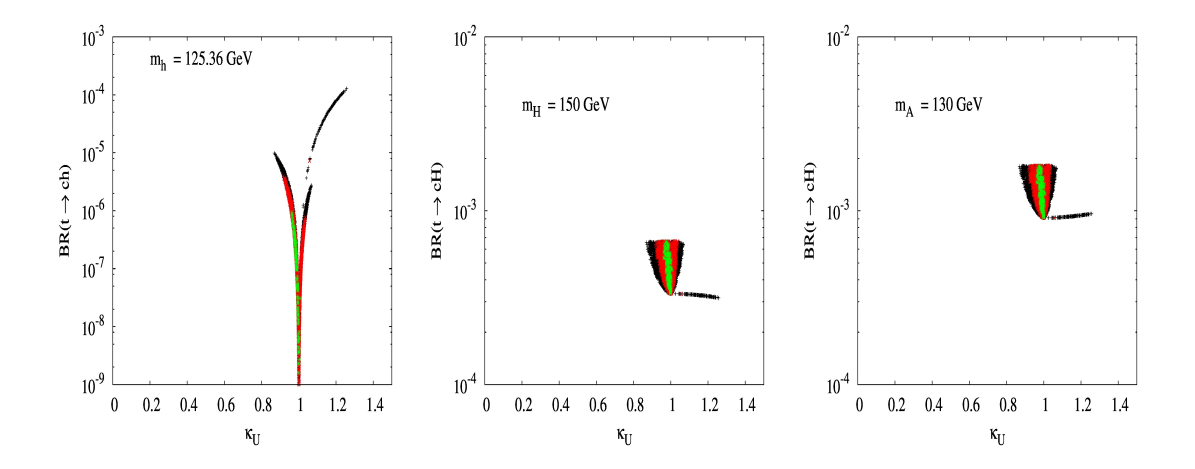


Figure 10. The legend is the same as 9 but for $\chi_F = -1$.

7 Conclusions

For studying the constraints of 8 TeV LHC experimental data, we perform χ -square analysis to find the most favorable regions for the free parameters in the two-Higgs-doublet models. For comparisons, we focus on the type-II and type-III models, in which the latter model not only affects the flavor conserving Yukawa couplings, but also generates the scalar-mediated flavor changing neutral currents at the tree level.

Although the difference between type-III and type-III is the Yukawa sector, however, since the new Yukawa couplings in type-III are associated with $\cos(\beta - \alpha)$ and $\sin(\beta - \alpha)$, the modified couplings tth and btH^{\pm} will change the constraint of free parameters.

In order to present the influence of modified Yukawa couplings, we show the allowed values of $\sin \alpha$ and $\tan \beta$ in Fig. 1, where the LHC updated data for $pp \to h \to f$ with $f = \gamma \gamma$, WW^*/ZZ^* and $\tau^+\tau^-$ are applied and other bounds are also included. By the results, we see that $\sin \alpha$ and $\tan \beta$ in type-III gets even stronger constraint if the dictated parameter $\chi_F = -1$ is adopted; on the contrary, if we take $\chi_F = +1$, the allowed values for $\sin \alpha$ and $\tan \beta$ are wider. It has been pointed out that there exist the wrong sign Yukawa couplings to down type quarks in the type-II model, i.e. $\sin \alpha > 0$ or $\kappa_D < 0$. By the study, we find that except the allowed regions of parameters are shrunk slightly, the situation in $\chi_F = -1$ is similar to the type-II case. In $\chi_F = +1$, although the $\kappa_D < 0$ is not excluded completely yet, but the case has a strict limit by current data. We show the analyses in Figs. 3 and 4. In these figures, one can also see the correlations of modified Higgs coupling to top-quark κ_U and to gauge boson κ_V .

When the parameters are bounded by the observed channels, we show the influence on the unobserved channel $h \to Z\gamma$ by using the scaling factor $\kappa_{Z\gamma}$, which is defined by the ratio of decay rate to the SM prediction. We find that the change of $\kappa_{Z\gamma}$ in type-III with $\chi_F = -1$ is less than 10%; however, with $\chi_F = +1$, the value of $\kappa_{Z\gamma}$ could be lower from SM prediction by over 10%. We also show our predictions for signal strengths $\mu_{\gamma\gamma}$ and $\mu_{\gamma Z}$ and their correlation at $\sqrt{s} = 13$ TeV.

The main difference between type-II and -III model is: the flavor changing neutral currents in the former are only induced by loops, while in the latter they could occur at the tree level. We study the scalar-mediated $t \to c(h, H, A)$ decays in type-III model and find that when all current experimental constraints are considered, $Br(t \to c(h, H)) < 10^{-3}$ for $m_h = 125.36$ and $m_H = 150$ GeV and $Br(t \to cA)$ slightly exceeds 10^{-3} for $m_A = 130$ GeV. The detailed numerical analyses are shown in Figs. 8, 9 and 10.

Acknowledgments

The authors thanks Rui Santos for useful discussions. A.A would like to thank NCTS for warm hospitality where part of this work has been done. The work of CHC is supported by the Ministry of Science and Technology of R.O.C under Grant #: MOST-103-2112-006-004-MY3. This work was also supported by the Moroccan Ministry of Higher Education and Scientific Research MESRSFC and CNRST: "Projet dans les domaines prioritaires de la recherche scientifique et du développement technologique": PPR/2015/6.

References

- [1] G. Aad *et al.* [ATLAS Collaboration], "Observation of a new particle in the search for the Standard Model Higgs boson with the ATLAS detector at the LHC", Phys. Lett. B **716**, 1 (2012) [arXiv:1207.7214 [hep-ex]].
- [2] S. Chatrchyan *et al.* [CMS Collaboration], "Observation of a new boson at a mass of 125 GeV with the CMS experiment at the LHC", Phys. Lett. B **716**, 30 (2012) [arXiv:1207.7235 [hep-ex]].
- [3] G. Aad et al. [ATLAS Collaboration], ATLAS note: ATLAS-CONF-2015-007
- [4] G. Aad et al. [ATLAS Collaboration].
- [5] ATALS Collaboration, ATLAS-CONF-2013-034.
- [6] S. Chatrchyan et al. . [CMS Collaboration], CMS-PAS-HIG-13-001.
- [7] S. Chatrchyan et al. . [CMS Collaboration], CMS-PAS-HIG-14-009
- [8] S. Dawson et al., "Working Group Report: Higgs Boson", arXiv:1310.8361 [hep-ex];
 D. Zeppenfeld, R. Kinnunen, A. Nikitenko and E. Richter-Was, "Measuring Higgs boson couplings at the CERN LHC", Phys. Rev. D 62 (2000) 013009 [hep-ph/0002036]; F. Gianotti and M. Pepe-Altarelli, "Precision physics at the LHC", Nucl. Phys. Proc. Suppl. 89 (2000) 177 [hep-ex/0006016].
- [9] C. Englert et al., "Precision Measurements of Higgs Couplings: Implications for New Physics Scales", J. Phys. G 41 (2014) 113001 [arXiv:1403.7191 [hep-ph]];
- [10] G. Moortgat-Pick et al., "Physics at the e^+e^- Linear Collider", arXiv:1504.01726 [hep-ph].
- [11] A. Arhrib, R. Benbrik and C. -H. Chen, "H → γγ in the Complex Two Higgs Doublet Model", arXiv:1205.5536 [hep-ph]; A. Arhrib, R. Benbrik, M. Chabab, G. Moultaka and L. Rahili, "hγγ Coupling in Higgs Triplet Model", arXiv:1202.6621 [hep-ph]; A. Arhrib, R. Benbrik and N. Gaur, "H → γγ in Inert Higgs Doublet Model", Phys. Rev. D 85, 095021 (2012) [arXiv:1201.2644 [hep-ph]]; A. Arhrib, R. Benbrik, M. Chabab, G. Moultaka and

- L. Rahili, "Higgs boson decay into 2 photons in the type II Seesaw Model", JHEP **1204**, 136 (2012) [arXiv:1112.5453 [hep-ph]].
- [12] C. W. Chiang and K. Yagyu, "Higgs boson decays to $\gamma\gamma$ and $Z\gamma$ in models with Higgs extensions", Phys. Rev. D **87**, no. 3, 033003 (2013) [arXiv:1207.1065 [hep-ph]]. C. S. Chen, C. Q. Geng, D. Huang and L. H. Tsai, " $h \to Z\gamma$ in Type-II seesaw neutrino model", Phys. Lett. B **723**, 156 (2013) [arXiv:1302.0502 [hep-ph]]. C. S. Chen, C. Q. Geng, D. Huang and L. H. Tsai, "New Scalar Contributions to $h \to Z\gamma$ ", Phys. Rev. D **87**, 075019 (2013) [arXiv:1301.4694 [hep-ph]].
- [13] T. D. Lee, "A Theory of Spontaneous T Violation", Phys. Rev. D 8, 1226 (1973); T. D. Lee, "CP Nonconservation and Spontaneous Symmetry Breaking", Phys. Rept. 9, 143 (1974).
- [14] J. F. Gunion, H. E. Haber, G. Kane and S. Dawson, "The Higgs HunterâÅŹs Guide" (Frontiers in Physics series, Addison-Wesley, 1990);
- [15] G. C. Branco, P. M. Ferreira, L. Lavoura, M. N. Rebelo, M. Sher and J. P. Silva, "Theory and phenomenology of two-Higgs-doublet models", Phys. Rept. 516, 1 (2012) [arXiv:1106.0034 [hep-ph]].
- [16] P.M. Ferreira, R. Santos, M. Sher and J.P. Silva, "Implications of the LHC two-photon signal for two-Higgs-doublet models", Phys. Rev. D 85, 077703 (2012) [arXiv:1112.3277 [hep-ph]];
 D. Carmi, A. Falkowski, E. Kuflik and T. Volansky, "Interpreting LHC Higgs Results from Natural New Physics Perspective", JHEP 1207 (2012) 136 [arXiv:1202.3144 [hep-ph]];
 H.S. Cheon and S.K. Kang, "Constraining parameter space in type-II two-Higgs doublet model in light of a 125 GeV Higgs boson", JHEP 1309, 085 (2013) [arXiv:1207.1083 [hep-ph]];
 W. Altmannshofer, S. Gori and G.D. Kribs, "A Minimal Flavor Violating 2HDM at the LHC", Phys. Rev. D 86, 115009 (2012) [arXiv:1210.2465 [hep-ph]];
 Y. Bai, V. Barger, L.L. Everett and G. Shaughnessy, "General two Higgs doublet model (2HDM-G) and Large Hadron Collider data", Phys. Rev. D 87, 115013 (2013) [arXiv:1210.4922 [hep-ph]];
 C.-Y. Chen and S. Dawson, "Exploring Two Higgs Doublet Models Through Higgs Production", Phys. Rev. D 87, 055016 (2013) [arXiv:1301.0309 [hep-ph]];
- [17] C-W. Chiang and K. Yagyu, "Implications of Higgs boson search data on the two-Higgs doublet models with a softly broken Z₂ symmetry", JHEP 1307, 160 (2013)
 [arXiv:1303.0168 [hep-ph]]; M. Krawczyk, D. Sokolowska and B. Swiezewska, "2HDM with Z₂ symmetry in light of new LHC data", J. Phys. Conf. Ser. 447, 012050 (2013)
 [arXiv:1303.7102 [hep-ph]]; B. Grinstein and P. Uttayarat, "Carving Out Parameter Space in Type-II Two Higgs Doublets Model", JHEP 1306, 094 (2013) [Erratum-ibid. 1309, 110 (2013)] [arXiv:1304.0028 [hep-ph]]; A. Barroso, P.M. Ferreira, R. Santos, M. Sher and J.P. Silva, "2HDM at the LHC the story so far", arXiv:1304.5225 [hep-ph]; B. Coleppa, F. Kling and S. Su, "Constraining Type II 2HDM in Light of LHC Higgs Searches", JHEP 1401, 161 (2014) [arXiv:1305.0002 [hep-ph]];
- [18] P.M. Ferreira, R. Santos, M. Sher and J.P. Silva, "2HDM confronting LHC data", arXiv:1305.4587 [hep-ph]; O. Eberhardt, U. Nierste and M. Wiebusch, "Status of the two-Higgs-doublet model of type II", JHEP 1307, 118 (2013) [arXiv:1305.1649 [hep-ph]]; S. Choi, S. Jung and P. Ko, "Implications of LHC data on 125 GeV Higgs-like boson for the Standard Model and its various extensions", JHEP 1310 (2013) 225 [arXiv:1307.3948 [hep-ph]].
- [19] V. Barger, L.L. Everett, H.E. Logan and G. Shaughnessy, "Scrutinizing h(125) in Two Higgs Doublet Models at the LHC, ILC, and Muon Collider", Phys. Rev. D 88 (2013) 115003

- [arXiv:1308.0052 [hep-ph]]; D. López-Val, T. Plehn and M. Rauch, "Measuring extended Higgs sectors as a consistent free couplings model", JHEP **1310** (2013) 134 [arXiv:1308.1979 [hep-ph]]; S. Chang, S.K. Kang, J.-P. Lee, K.Y. Lee, S.C. Park and J. Song, "Two Higgs doublet models for the LHC Higgs boson data at $\sqrt{s} = 7$ and 8 TeV", arXiv:1310.3374 [hep-ph]; K. Cheung, J. S. Lee and P. -Y. Tseng, "Higgcision in the Two-Higgs Doublet Models", JHEP **1401**, 085 (2014) [arXiv:1310.3937 [hep-ph]]; A. Celis, V. Ilisie and A. Pich, "Towards a general analysis of LHC data within two-Higgs-doublet models", JHEP **1312**, 095 (2013) [arXiv:1310.7941 [hep-ph]];
- [20] L. Wang and X. F. Han, "Status of the aligned two-Higgs-doublet model confronted with the Higgs data", JHEP 1404, 128 (2014) [arXiv:1312.4759 [hep-ph]]; K. Cranmer, S. Kreiss, D. López-Val and T. Plehn, "A Novel Approach to Higgs Coupling Measurements", arXiv:1401.0080 [hep-ph]; F. J. Botella, G. C. Branco, A. Carmona, M. Nebot, L. Pedro and M. N. Rebelo, "Physical Constraints on a Class of Two-Higgs Doublet Models with FCNC at tree level", JHEP 1407, 078 (2014) [arXiv:1401.6147 [hep-ph]]; F. J. Botella, G. C. Branco, M. Nebot and M. N. Rebelo, "Flavour Changing Higgs Couplings in a Class of Two Higgs Doublet Models", arXiv:1508.05101 [hep-ph]. S. Kanemura, K. Tsumura, K. Yagyu and H. Yokoya, "Fingerprinting non-minimal Higgs sectors", arXiv:1406.3294 [hep-ph];
- [21] A. Celis, V. Ilisie and A. Pich, "LHC constraints on two-Higgs doublet models", arXiv:1302.4022 [hep-ph]; P. M. Ferreira, H. E. Haber, R. Santos and J. P. Silva, "Mass-degenerate Higgs bosons at 125 GeV in the Two-Higgs-Doublet Model", arXiv:1211.3131 [hep-ph]; A. Barroso, P. M. Ferreira, R. Santos and J. P. Silva, "Probing the scalar-pseudoscalar mixing in the 125 GeV Higgs particle with current data", Phys. Rev. D 86, 015022 (2012) [arXiv:1205.4247 [hep-ph]]; P. M. Ferreira, R. Santos, M. Sher and J. P. Silva, "Could the LHC two-photon signal correspond to the heavier scalar in two-Higgs-doublet models?", Phys. Rev. D 85, 035020 (2012) [arXiv:1201.0019 [hep-ph]]. P. M. Ferreira, R. Santos, M. Sher and J. P. Silva, "Implications of the LHC two-photon signal for two-Higgs-doublet models", Phys. Rev. D 85, 077703 (2012) [arXiv:1112.3277 [hep-ph]]. A. E. Carcamo Hernandez, R. Martinez and J. A. Rodriguez, Eur. Phys. J. C 50 (2007) 935 [hep-ph/0606190]. A. Crivellin, A. Kokulu and C. Greub, Phys. Rev. D 87 (2013) 9, 094031 [arXiv:1303.5877 [hep-ph]]. A. Crivellin, J. Heeck and P. Stoffer, arXiv:1507.07567 [hep-ph].
- [22] A. Arhrib, M. Capdequi Peyranere, W. Hollik and S. Penaranda, "Higgs decays in the two Higgs doublet model: Large quantum effects in the decoupling regime", Phys. Lett. B **579**, 361 (2004) [hep-ph/0307391].
- [23] D. Fontes, J. C. Romãco and J. P. Silva, Phys. Rev. D 90, 015021 (2014) [arXiv:1406.6080 [hep-ph]]. G. Bhattacharyya, D. Das, P. B. Pal and M. N. Rebelo, JHEP 1310, 081 (2013) [arXiv:1308.4297 [hep-ph]].
- [24] J. A. Aguilar-Saavedra, "Top flavour-changing neutral interactions: Theoretical expectations and experimental detection", Acta Phys. Polon. B 35, 2695 (2004) [arXiv:hep-ph/0409342].
- [25] G. Eilam, J. L. Hewett and A. Soni, "Rare Decays Of The Top Quark In The Standard And Two Higgs Doublet Models", Phys. Rev. D 44 (1991) 1473 [Erratum-ibid. D 59 (1999) 039901].
- [26] ATLAS Collaboration, ATL-PHYS-PUB-2013-012 (2013); ATLAS Collaboration, ATLAS-CONF-2013-081.
- [27] CMS Collaboration, CMS-PAS-HIG-13-034 (2014).

- [28] S. L. Glashow and S. Weinberg, "Natural Conservation Laws For Neutral Currents", Phys. Rev. D 15 (1977) 1958.
- [29] T. P. Cheng and M. Sher, "Mass Matrix Ansatz and Flavor Nonconservation in Models with Multiple Higgs Doublets", Phys. Rev. D 35, 3484 (1987).
- [30] D. Atwood, L. Reina and A. Soni, "Phenomenology of two Higgs doublet models with flavor changing neutral currents", Phys. Rev. D 55, 3156 (1997) [hep-ph/9609279]; C. -H. Chen and C. -Q. Geng, "Scalar interactions to the polarizations of B —> phi K*", Phys. Rev. D 71, 115004 (2005) [hep-ph/0504145].
- [31] M. Gomez-Bock and R. Noriega-Papaqui, "Flavor violating decays of the Higgs bosons in the THDM-III", J. Phys. G 32, 761 (2006) [hep-ph/0509353]; M. Gomez-Bock, G. Lopez Castro, L. Lopez-Lozano and A. Rosado, "Flavor-changing neutral current in production and decay of pseudoscalar mesons in a type III two-Higgs-doublet-model with four-texture Yukawa couplings", Phys. Rev. D 80, 055017 (2009) [arXiv:0905.3351 [hep-ph]].
- [32] J. F. Gunion and H. E. Haber, "The CP conserving two Higgs doublet model: The Approach to the decoupling limit", Phys. Rev. D 67, 075019 (2003) [hep-ph/0207010].
- [33] I. F. Ginzburg, M. Krawczyk and P. Osland, "Resolving SM like scenarios via Higgs boson production at a photon collider. 1. 2HDM versus SM", In *2nd ECFA/DESY Study 1998-2001* 1705-1733 [hep-ph/0101208]. I. F. Ginzburg, M. Krawczyk and P. Osland, "Potential of photon collider in resolving SM like scenarios", Nucl. Instrum. Meth. A 472, 149 (2001) [hep-ph/0101229].
- [34] A. G. Akeroyd, A. Arhrib and E. M. Naimi, "Note on tree-level unitarity in the general two Higgs doublet model", Phys. Lett. B 490, 119 (2000) [arXiv:hep-ph/0006035]. A. Arhrib, "Unitarity constraints on scalar parameters of the standard and two Higgs doublets model", arXiv:hep-ph/0012353.
- [35] S. Kanemura, T. Kubota and E. Takasugi, "Lee-Quigg-Thacker bounds for Higgs boson masses in a two doublet model", Phys. Lett. B 313, 155 (1993) [arXiv:hep-ph/9303263].
 J. Horejsi and M. Kladiva, "Tree-unitarity bounds for THDM Higgs masses revisited", Eur. Phys. J. C 46, 81 (2006) [arXiv:hep-ph/0510154].
- [36] M. Sher, "Electroweak Higgs Potentials And Vacuum Stability", Phys. Rept. 179, 273 (1989). S. Kanemura, T. Kasai and Y. Okada, "Mass bounds of the lightest CP-even Higgs boson in the two-Higgs-doublet model", Phys. Lett. B 471, 182 (1999) [arXiv:hep-ph/9903289].
- [37] P. M. Ferreira, R. Santos and A. Barroso, "Stability of the tree-level vacuum in two Higgs doublet models against charge or CP spontaneous violation", Phys. Lett. B 603, 219 (2004) [arXiv:hep-ph/0406231].
- [38] M. E. Peskin and T. Takeuchi, "Estimation of oblique electroweak corrections", Phys. Rev. D 46 (1992) 381.
- [39] M. Baak *et al.* [Gfitter Group Collaboration], "The global electroweak fit at NNLO and prospects for the LHC and ILC", Eur. Phys. J. C **74** (2014) 3046 [arXiv:1407.3792 [hep-ph]].
- [40] M. Misiak *et al.*, "Updated NNLO QCD predictions for the weak radiative B-meson decays", Phys. Rev. Lett. **114**, no. 22, 221801 (2015) [arXiv:1503.01789 [hep-ph]].
- [41] M. Baak, M. Goebel, J. Haller, A. Hoecker, D. Ludwig, K. Moenig, M. Schott and J. Stelzer, "Updated Status of the Global Electroweak Fit and Constraints on New Physics", Eur.

- Phys. J. C **72**, 2003 (2012) [arXiv:1107.0975 [hep-ph]]. H. E. Haber and H. E. Logan, "Radiative corrections to the Z b anti-b vertex and constraints on extended Higgs sectors", Phys. Rev. D **62**, 015011 (2000) [hep-ph/9909335].
- [42] A. Djouadi, "The Anatomy of electro-weak symmetry breaking. I: The Higgs boson in the standard model", Phys. Rept. 457 (2008) 1 [hep-ph/0503172]. A. Djouadi, "The Anatomy of electro-weak symmetry breaking. II. The Higgs bosons in the minimal supersymmetric model", Phys. Rept. 459, 1 (2008) [hep-ph/0503173].
- [43] CMS Collaboration, CMS-PAS-HIG-13-005.
- [44] D. M. Asner, T. Barklow, C. Calancha, K. Fujii, N. Graf, H. E. Haber, A. Ishikawa and S. Kanemura *et al.*, "ILC Higgs White Paper", arXiv:1310.0763 [hep-ph].
- [45] A. Arhrib,"Top and Higgs flavor changing neutral couplings in two Higgs doublets model", Phys. Rev. D 72, 075016 (2005) [hep-ph/0510107]. I. Baum, G. Eilam and S. Bar-Shalom, Phys. Rev. D 77, 113008 (2008) [arXiv:0802.2622 [hep-ph]]. S. Bejar, J. Guasch and J. Sola, Nucl. Phys. B 600 (2001) 21 [hep-ph/0011091].
- [46] B. Altunkaynak, W. S. Hou, C. Kao, M. Kohda and B. McCoy, "Flavor Changing Heavy Higgs Interactions at the LHC", arXiv:1506.00651 [hep-ph].